



Drift Rather than Selection Dominates MHC Class II Allelic Diversity Patterns at the Biogeographical Range Scale in Natterjack Toads *Bufo calamita*

Inga Zeisset^{1,2*}, Trevor J. C. Beebee²

1 School of Pharmacy and Biomolecular Sciences, University of Brighton, Brighton, United Kingdom, **2** School of Life Sciences, University of Sussex, Brighton, United Kingdom

Abstract

Study of major histocompatibility complex (MHC) loci has gained great popularity in recent years, partly due to their function in protecting vertebrates from infections. This is of particular interest in amphibians on account of major threats many species face from emergent diseases such as chytridiomycosis. In this study we compare levels of diversity in an expressed MHC class II locus with neutral genetic diversity at microsatellite loci in natterjack toad (*Bufo (Epidalea) calamita*) populations across the whole of the species' biogeographical range. Variation at both classes of loci was high in the glacial refugium areas (REF) and much lower in postglacial expansion areas (PGE), especially in range edge populations. Although there was clear evidence that the MHC locus was influenced by positive selection in the past, congruence with the neutral markers suggested that historical demographic events were the main force shaping MHC variation in the PGE area. Both neutral and adaptive genetic variation declined with distance from glacial refugia. Nevertheless, there were also some indications from differential isolation by distance and allele abundance patterns that weak effects of selection have been superimposed on the main drift effect in the PGE zone.

Citation: Zeisset I, Beebee TJC (2014) Drift Rather than Selection Dominates MHC Class II Allelic Diversity Patterns at the Biogeographical Range Scale in Natterjack Toads *Bufo calamita*. PLoS ONE 9(6): e100176. doi:10.1371/journal.pone.0100176

Editor: Sofia Consuegra, Swansea University, United Kingdom

Received: July 2, 2013; **Accepted:** May 23, 2014; **Published:** June 17, 2014

Copyright: © 2014 Zeisset, Beebee. This is an open-access article distributed under the terms of the Creative Commons Attribution License, which permits unrestricted use, distribution, and reproduction in any medium, provided the original author and source are credited.

Funding: This research was funded by the Leverhulme trust (<http://www.leverhulme.ac.uk>). Grant number: F/00230/AH. The funders had no role in study design, data collection and analysis, decision to publish, or preparation of the manuscript.

Competing Interests: The authors have declared that no competing interests exist.

* E-mail: i.zeisset@brighton.ac.uk

Introduction

The basis of adaptive rather than neutral genetic variation has become increasingly accessible in recent years as loci under selection are identified and characterised. Some of the most popular genes used in this context are those belonging to the major histocompatibility complex (MHC). These genes play an important role in the adaptive immune response of vertebrates. MHC class I molecules present intracellular pathogen peptides to CD8+ T lymphocytes (T cells), primarily in response to viral infections, whereas MHC class II molecules (composed of α and β subunits) present extracellular pathogen peptides to CD4+ T cells after invasion by bacteria and fungi [1]. Although there is some variation among vertebrates in MHC gene structure, MHC class II β genes in the amphibian *Xenopus laevis* are made up of six exons with an exon-intron organization similar to that of a typical mammalian class II β gene. Exon 2 encodes the β - 1 domain which includes most of the antigen binding sites (ABS) of the beta domain and is the most polymorphic region of the gene [2], [3]. Due to high selective pressure on MHC genes, variation tends to be high, particularly at the ABS [4]. These sites encode amino acid residues involved in the recognition and binding of foreign peptides [5].

Frequency dependent selection, where bearers of common alleles are likely to be more susceptible to diseases and specific alleles can confer resistance [6], [7] or heterozygote advantage [8], [9] are believed to be common mechanisms involved in shaping

MHC diversity. Low diversity at MHC loci has been implicated in elevating vulnerability to disease [10], [11], though several species have not shown demonstrable ill effects from limited MHC variation [12], [13]. Single MHC class I or II alleles confer resistance to specific diseases in many taxa [14], [15], [16] and some studies suggest that it is the prevalence of parasites which maintain high levels of MHC variation [17], [18], [19]. However, in many cases stochastic events, rather than selection influence MHC variation and variation at neutral markers is often correlated with that of MHC loci, e.g. [11], [20], [21]. The mechanisms driving MHC evolution have therefore not been fully resolved. Natural selection, demographic processes such as drift and gene flow as well as mutation rate are all likely to play a role.

Few studies have investigated MHC variation and neutral genetic variation across entire biographical ranges of species and most of these involve only few populations or species within limited ranges [12], [22], [23], [24], [25], [26]. It is therefore particularly interesting to compare diversity at neutral markers and functionally important genes in species at wide biogeographical scales. In particular, species with large ranges and which have been subjected to population bottlenecks in areas of their distribution are ideal for comparisons of neutral and adaptive genetic variation. Postglacial expansion of amphibians from glacial refugia provides useful examples. Most European species survived the last glaciations, peaking around 20,000 years ago, in southern refugia from which they subsequently colonised northern Europe in the

postglacial Holocene period [27]. Furthermore, amphibians are experiencing high rates of global decline [28], [29], mainly due to habitat degradation and loss [30] but also because of emerging infectious diseases such as the chytrid fungus *Batrachochytrium dendrobatidis* (Bd, [31]). This pathogen precipitated the decline of at least two species in parts of Iberia [32], but many other infected species appear largely unaffected [33], [34], [35]. As MHC class II molecules play an important role in mounting acquired immune responses to fungi, and MHC variability is often associated with immunocompetence [36], it is likely that MHC-dependent resistance mechanisms contribute to fighting Bd infections [37]. A recent study on leopard frogs, for example, showed an association between MHC class II genotypes and survival of Bd infections [38]. Information on MHC loci, and MHC class II β 1 genes in particular, is now available for several amphibians including members of the genus *Bombina*, *Alytes* [39], *Rana* [40], [41], *Bufo* [42], [43], *Espadarana* and *Sachatamia* [44] and *Triturus* [12], [45], as well as for model organisms such as *Xenopus*, *Silurana* and *Ambystoma* [46], [47], [48], [49].

Here we report the results of a study of MHC and microsatellite diversity across the entire biogeographical range of *Bufo calamita*, an amphibian with glacial refugia in Iberia and south-west France, which now also inhabits much of north and central Europe [50]. We recently characterized the entire exon 2 of an expressed MHC class II β locus (locus B, [43]) in *B. calamita* and here we provide evidence that this locus is or has been under selection in this species. We then tested the hypothesis that effects of selection on this locus during postglacial expansion resulted in patterns of diversity different from those of microsatellites, which were presumed to be primarily consequent on genetic drift.

Materials and Methods

Sampling Strategy

For MHC analyses we extracted DNA from 325 individuals from 17 populations of *B. calamita* distributed over the entire species' range (see Figure 1 and Table 1). Thirteen of those populations were used in previous studies of microsatellite diversity [50], [51] but samples from five further populations used in those studies were no longer available (grey circles in Figure 1). We therefore supplemented the study with samples from four new sites (white circles in Figure 1) to maintain coverage of the full biogeographic range. In all cases free swimming tadpoles (Gosner stages 25–30) were sampled and instantly sacrificed by immersion in ethanol (a method approved by the British Home Office). All UK samples were authorized and licensed by Natural England, the statutory government organisation responsible for wildlife conservation. *Bufo calamita* is a protected species in Britain and in some of the other countries providing samples. In all cases the appropriate permissions were obtained by the samplers in those countries. *Bufo calamita* is a vertebrate but no ethical permissions were required for this study because it only required instant sacrifice of larvae, which does not come under ethical coding since no manipulations, mutilations or other stresses were applied. DNA extractions were performed as described in Zeisset & Beebee [40]. Four of the 17 populations were located in the glacial refugium area (REF, as per [12]) of Iberia and southern France, while the other 13 were located in the postglacial expansion area (PGE, as per [12]), all as inferred from mtDNA haplotype diversity [50].

MHC Genotyping

MHC class II locus B β chain exon 2 sequences of *B. calamita* were amplified using primers located in the flanking intron regions. This is the only functional MHC class II locus thus far

identified in *B. calamita* [42], [43]. The forward primer 2F347 (GTGACCCCTCTGCTCTCCATT) with reverse primer 2R307b (ATAATTCAGTATATACAGGGTCTCACC) amplified a sequence of 279–282 base pairs (excluding primers). The 20 μ l PCRs contained approximately 25 ng DNA, 0.4 μ M of each primer, 100 μ M dNTPs, 1x reaction buffer and 0.5 U of New England Biolabs *Taq* DNA polymerase. Thermal cycling consisted of an initial denaturation step of 94°C for 3 min and a touchdown protocol with a total of 35 cycles and ending with an elongation step of 72°C for 10 min. Each cycle started with a denaturation step of 94°C for 30 sec and ended with an elongation step of 72°C for 40 sec. Annealing temperatures consisted of 2 cycles at 62°C, 2 cycles at 60°C, 2 cycles at 58°C and 29 cycles at 56°C, each for 30 sec. Individual alleles were identified by SSCP analysis as described in Zeisset & Beebee [40]. Bands were excised from gels, re-amplified following Sunnucks *et al.* [52] and sent away for sequencing (Macrogen, Korea or Oxford Biochemistry Dept, UK). To reduce the risk of including PCR artefacts each allele was sequenced at least twice, either from different individuals or from two separate PCRs.

Microsatellite Data

For comparative purposes we used microsatellite data obtained in previous studies from eight polymorphic loci in 600 individuals sampled from 18 populations [50], [51] and distributed over the entire biogeographical range (Figure 1, Table 1). To minimize PCR and scoring errors a small subset of samples with high incidences of non-amplification or difficult to score alleles were run twice. Microsatellite data were tested for the presence of null alleles and scoring errors using Micro-Checker 2.2.3 [53] and for effects of selection using the F_{ST} outlier approach implemented in LOSITAN [54], [55].

MHC Sequence Analysis

To determine intron/exon boundaries we combined the putative intron and exon sequences (Genbank nos.: JX258913 and JX258914) to obtain a 532 base pair sequence of *B. calamita* locus B allele 'Buca B2' and used NNSPLICE version 0.9 [56], as implemented on http://www.fruitfly.org/seq_tools/splice.html, to predict splice sites.

Sequences were aligned and edited manually using Bioedit v. 7.0.9 [57]. The relative rates of non-synonymous (dN) and synonymous (dS) base pair substitutions were calculated according to Nei & Gojobori [58] applying the Jukes Cantor correction [59] for multiple hits in Mega 5 [60]. This was done for all sites and just for putative antigen binding sites (ABS), assuming functional congruence to human ABS identified by Tong *et al.* [61]. We used a Z-test [62] for positive selection. We also calculated average pairwise nucleotide distances (Kimura 2-parameter model, K2P) and Poisson-corrected amino acid distances [63] for ABS, non-ABS and all sites in Mega 5 with 1000 bootstrap replicates to calculate standard errors for the distance measures.

To identify specific sites under selection we used two new methods: a mixed effects model of evolution (MEME) to identify instances of both episodic and transient positive selection at individual sites [64] as well as a fast unbiased Bayesian approximation (FUBAR), both implemented on <http://www.datamonkey.org> [65]. MEME is superior at detecting sites where episodic positive selection is likely to be occurring [64]. For these analyses we used 282 bp (94 amino acids) of 57 locus B alleles of three species, *B. calamita*, *Bufo bufo* and *Bufo (Pseudoepidalea) viridis* (Genbank nos.: HQ388288, HQ388291, JX258874–JX258913, JX046488–JX046501, JX258919). After testing for recombina-

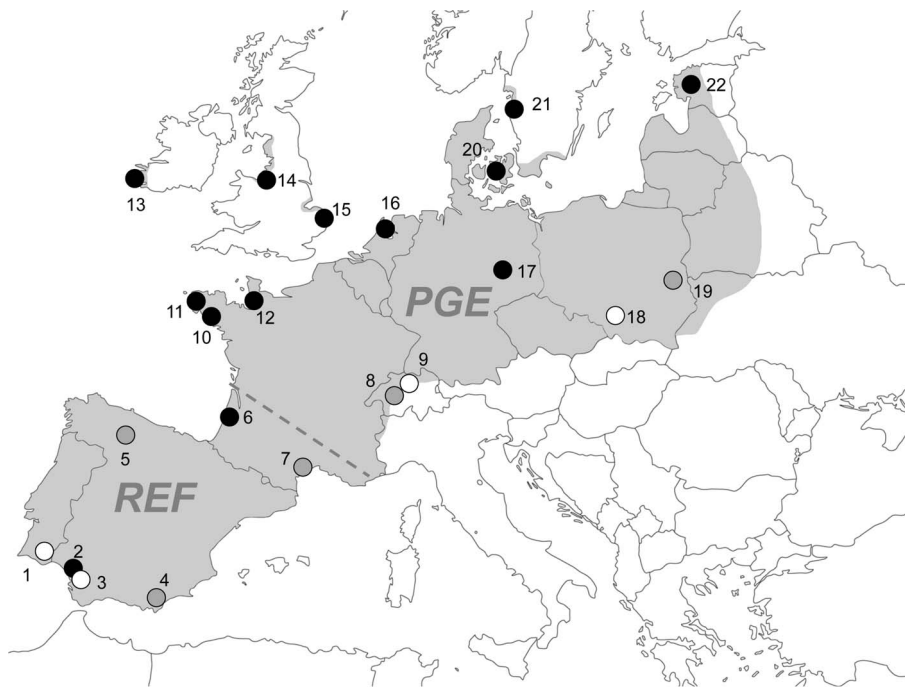


Figure 1. Natterjack toad distribution and sampling sites for microsatellite and MHC analyses. Dark shading indicates natterjack toad distribution in Europe. Black circles indicate sites for which both MHC and microsatellite data was collected, white circles indicate MHC data only and grey circles microsatellite data only. Sampling sites (area or nearest town) were: 1. Algarve, Portugal; 2. Seville, Spain; 3. Doñana, Spain; 4. Almeria, Spain; 5. Leon, Spain; 6. Bordeaux, France; 7. Carmargue, France; 8 and 9 near Zurich, Switzerland; 10. Carnac, France; 11. Penmarch, France; 12. Cherbourg, France; 13. Kerry, Ireland; 14. Birkdale, UK; 15. Winterton, UK; 16. Texel, Netherlands; 17. Halle, Germany; 18. Bukowno, Poland; 19. Bielowieza, Poland; 20. Zealand, Denmark; 21. Uddevalla, Sweden; 22. Parnu, Estonia. The dashed line indicates the approximate division between the glacial refugia (REF) and postglacial expansion (PGE) areas. Map modified from d-maps.com.
doi:10.1371/journal.pone.0100176.g001

tion, a phylogenetic tree was inferred and used as the input for selection on particular codons using the two methods.

To investigate the evolutionary relationship between the MHC loci in the three *Bufo* species we used three methods were to test for signatures of recombination. This analysis was carried out for 282 bp of exon 2 sequence as well as for the 157 bp we used in phylogenetic tree reconstruction to investigate the effects recombination may have on tree construction. For this analysis we also included *B. calamita*, *B. bufo* and *B. viridis* locus A alleles (locus A is a putative non-functional locus, identified in an earlier study [43], (Genbank nos.: JX258916, JX283352, JX283353, JX258920, JX046502–JX046504) and used GENECONV [66] and MaxChi2 [67], both implemented in RDP3.44 [68]. Both of these methods performed well in a comparison of 14 recombination detection methods [69]. We applied Bonferroni correction for multiple tests and used automask sequences to optimize our dataset and to reduce the severity of the multiple testing correction. In addition we used a genetic algorithm recombination detection method (GARD; [70]), as implemented on <http://www.datamonkey.org/GARD>.

MHC Phylogeny

We constructed a phylogenetic tree to visualize the relationship between anuran MHC class II β exon 2 alleles based on a total of 51 unique exon 2 sequences from 14 species: *Bufo bufo*, *B. viridis*, *Bombina orientalis*, *B. variagata*, *B. pachypus*, *Alytes obstetricans*, *Xenopus laevis*, *Rana temporaria*, *R. catesbeiana*, *R. yavapaiensis*, *R. clamitans*, *R. sylvatica*, *Saxatamia illex* and *Espadarana prosoblepon* [43], [39], [41], [2], [46], [44] in the NCBI database, in addition to a selection of our own from this study chosen to include the some of the most

diverse sequences. Sequences were trimmed to 157 bp to match available data from the published exon 2 sequences. The urodele *Ambystoma tigrinum* and *Triturus cristatus* MHC sequences were included as outgroups. To investigate the evolutionary relationship among the 38 *B. calamita* locus B sequences from this study we constructed another phylogenetic tree, using 282 bp of sequence and *X. laevis* as an outgroup. For both trees evolutionary history was inferred using the Maximum Likelihood method based on the Kimura 2-parameter model [71] in Mega 5 [60]. Other tree building methods were also tested and provided congruent results (data not shown). A consensus tree was inferred from 1000 replicates [72]. As recombination and possible gene duplication can affect phylogenetic trees we also constructed a phylogenetic network using the program SplitsTree4, which can account for conflicting signals from recombination and gene duplication [73], [74] for the *B. calamita* MHC class II locus B. We used Jukes-Cantor distances and the Neighbor-Net method. For a network depicting the relationship between all three *Bufo* species' MHC sequences see [43].

Population Genetics

Compliance with Hardy-Weinberg equilibrium (HWE) in each population was assessed for microsatellite and MHC loci by applying the exact tests in Genepop 4.0.10 [75]. Linkage disequilibrium of the microsatellite markers was also tested in Genepop.

F-statistics [76], pairwise multilocus permutation tests of population differentiation, expected heterozygosity (H_E) and allelic richness (i.e. the mean number of alleles corrected for samples size; R), were estimated for each population and overall in FSTAT

Table 1. Summary statistics for MHC and microsatellite loci.

Populations	Microsatellites										MHC									
	<i>N</i>	<i>N_{alleles}</i> (<i>SD</i>)	<i>N_p</i>	<i>R</i>	<i>H_E</i>	<i>N</i>	<i>N_{alleles}</i>	<i>N_p</i>	<i>R</i>	<i>H_E</i>										
<i>Postglacial expansion (PGE) areas:</i>																				
NW England (14)	40	2.1 (1.46)	0	2.0	0.30	29	2	0	2.0	0.49										
SE England (15)	39	2.4 (0.98)	0	2.1	0.34	24	2	0	2.0	0.50										
Ireland (13)	40	2.1 (1.35)	0	1.9	0.29	9	1	0	1.0	0.00										
NW France (10)	40	2.0 (1.16)	0	1.9	0.26	12	2	0	1.8	0.08										
NW France (11)	31	4.4 (1.62)	3	3.3	0.46	14	2	1	2.6	0.52										
NW France (12)	39	3.4 (1.51)	0	3.2	0.47	22	3	1	2.9	0.53										
Netherlands (16)	40	2.7 (1.70)	1	2.5	0.36	17	2	0	1.5	0.06										
Germany (17)	40	3.6 (2.44)	3	3.1	0.46	27	3	0	3.0	0.57										
Poland (18 & 19)	40	1.9 (0.69)	0	1.7	0.21	13	2	0	1.9	0.15										
Estonia (22)	37	1.4 (0.79)	1	1.4	0.14	21	1	0	1.0	0.00										
Denmark (20)	37	1.29 (0.49)	0	1.3	0.11	14	1	0	1.0	0.00										
Sweden (21)	40	1.7 (0.95)	0	1.5	0.14	24	2	0	2.0	0.51										
Switzerland (8 & 9)	40	2.86 (0.69)	1	2.7	0.50	30	5	3	3.5	0.60										
PGE means (SD)	38.7 (2.46)	2.5 (1.22)	0.69 (0.99)	2.2 (0.99)	0.31 (0.14)	19.7 (6.68)	2.2 (1.07)	0.38 (0.84)	2.0 (0.80)	0.31 (0.26)										
PGE total numbers	503	64	9	-	-	256	12	5	-	-										
<i>Refugia (REF) areas</i>																				
SW France (6)	16	5.3 (1.11)	5	4.6	0.67	13	5	2	5.6	0.81										
SE Spain (4)	11	4.7 (1.60)	1	4.5	0.68	-	-	-	-	-										
N Spain (5)	12	4.7 (1.11)	5	4.6	0.73	-	-	-	-	-										
SW Spain (2)	36	9.3 (2.56)	12	6.7	0.79	10	4	0	4.0	0.78										
SW Spain (3)	-	-	-	-	-	13	14	11	10.8	0.91										
Portugal (1)	-	-	-	-	-	33	12	8	7.6	0.84										
SE France (7)	22	5.9 (1.95)	3	4.9	0.65	-	-	-	-	-										
REF means (SD)	19.4 (9.16)	6.0 (1.67)	5.2 (3.65)	5.0 (0.93)	0.70 (0.06)	17.3 (9.18)	8.8 (4.99)	5.25 (4.43)	7 (2.93)	0.84 (0.06)										
REF total numbers	97	99	26	-	-	69	30	21	-	-										

Summary statistics for MHC and microsatellite loci of *B. calamita* populations. The numbers in the population column refer to sampling sites in Figure 1. *N* is sample size and *N_{alleles}* is mean number of alleles with standard deviations given for microsatellite loci; *N_p* is the number of population-specific alleles occurring only in one population, *R* is the allelic richness adjusted to the minimum sample size of nine individuals. *H_E* is mean expected heterozygosity.

doi:10.1371/journal.pone.0100176.t001

2.9.3.2 [77]. We used F_{ST} primarily as a way to measure the level of differentiation between populations. As F_{ST} may be affected by highly variable markers such as microsatellites we also calculated D_{EST} [78] in GenAlEx 6.5b3 [79], [80]. Pairwise comparisons of F_{ST} and D_{EST} within and between each class of loci, as well as isolation by distance (using \ln distance vs. $F_{ST}/1 - F_{ST}$), were made using the Mantel test facility in Genepop with 1000 permutations. Distances were measured using Google Earth between all sampling sites north of the Pyrenees (the region of postglacial expansion) that were not separated by sea, as most amphibians cannot survive seawater exposure. Distances were otherwise direct (Euclidean) allowing for bends to avoid sea water where necessary.

To investigate how variation was partitioned within and among REF and PGE populations we carried out an AMOVA in Arlequin v. 3.5 [81] for microsatellite and MHC data.

Phylogeographic relationships among the populations based on allele frequencies were determined separately for microsatellite and MHC data using Phylip v. 3.66 [82]. The analysis employed Cavalli-Sforza chord distances and the UPGMA algorithm with 1000 bootstraps for the multilocus microsatellite data.

Standard statistical tests for differences in allelic richness (R) and expected heterozygosity (H_E) between REF and PGE populations as well as correlations between microsatellite and MHC data and microsatellite and allelic richness (R) and geographic distance were carried out using Statistix7 (Analytical Software, Tallahassee, USA).

Results

MHC Locus B Characteristics

Splice site analysis for locus B predicted intron/exon boundaries between base pairs 3 and 4 after the 3' end of the forward primer binding site and between base pairs 281 and 282 (2 bp into the reverse primer binding site), making the putative exon 279 base pairs long. These sites corresponded to exon 2 boundaries found in some other amphibian species [39]. There was evidence of historical positive natural selection at ABS sites in *B. calamita* ($P = 0.002$, $Z = 2.973$). Using MEME ($P < 0.1$) we identified 23 positively selected codons in exon 2 and using FUBAR with a posterior probability $> 90\%$ we found 19. Codons identified by both methods largely corresponded to putative antigen binding sites (ABS) as defined by Brown *et al.* [83] and Tong *et al.* [61] for the human MHC locus HLA-DRB (Figure 2). Average nucleotide distance over all nucleotide sequence pairs in exon 2 was 0.094 (SE 0.012) in *B. calamita*. Average amino acid distance at this locus was 0.149 (SE 0.028). Nucleotide and amino acid distances were much higher in the putative ABS (nucleotide: 0.376, SE 0.067; amino acid: 0.787, SE 0.159) than in non-ABS (nucleotide: 0.058, SE 0.010; amino acid: 0.083, SE 0.021) sites.

Of the 38 unique MHC class II exon 2 DNA sequences (Genbank nos.: HQ3882288, HQ388289, JX258875–JX258911) from locus B in 17 populations of *B. calamita*, ten showed evidence of a recombination event including a codon insertion towards the 3' end resulting in the addition of threonine. Five had a deletion of three nucleotides which corresponded to a codon deletion in the MHC class II DAB alleles of the great crested newt, *Triturus cristatus* (Trcr-DAB*06, 08, 12, 15, 17, 19, 20 and 24, [84]) in Europe, as well as in the glass frog *Espadarana prosoblepon* (Espr-DRB*26, [44]) in Central America. In all three species phenylalanine or tyrosine was lost as well as a number of others in the case of the glass frog.

Recombination tests GeneConv and MaxChi detected between two and three recombination events among all the whole exon 2 MHC sequences, with between five and 15 recombination

signals. GARD on the other hand detected no evidence of recombination. For the 157 bp sequences used in phylogenetic tree reconstruction only MaxChi detected one recombination event, with 13 recombination signals.

Amphibian MHC class II exon 2 sequences formed some strongly supported clusters (Figure 3A). *Rana*, *Xenopus* and Discoglossidae (*Bombina* and *Alytes* species) sequences all formed separate groups. Within those groups there was also strong support for some branches separating species. The Central American *Sachatamia* and *Espadarana* clustered strongly with the European *Bufo*. Both the phylogenetic network (Figure S1) and the tree (Figure 3B) produced congruent results for the *B. calamita* MHC class II B locus.

Population Genetics

For the MHC locus there were a total of 12 alleles in 256 individuals in the PGE group, but 30 alleles in 69 individuals in the REF group. There was a remarkably high number of population-specific alleles (25 out of 38, 66%) in the MHC data, each of which was found in a single population (Table 1). Twenty six alleles (68%) including 20 population-specific alleles (80%) were only found in the REF group and eight alleles (five population-specific) only in the PGE group. Only four alleles (10%) occurred in both groups, though in the REF group they were only found in the SW France population and not in any of the Iberian populations. None of the alleles found in Iberia occurred north of the Pyrenees and vice versa. However, the alleles in the REF and PGE groups did not cluster as similar sequences (Figure 3B) implying a common ancient ancestry for the alleles occurring in both groups combined. Three of the 17 populations (Germany, Spain (Doñana) and Portugal) were not in HWE at the MHC locus, in all cases due to a homozygote excess. As selection can generate divergence from HWE, we did not exclude these populations from further analysis. Although the presence of null alleles could not be ruled out, the fact that the primers were located in relatively conserved intron sequences means that null alleles are unlikely to be the cause of the deviation from HWE. Among the microsatellites LOSITAN identified one locus (Bcal μ 8) as possibly affected by positive selection and we therefore excluded this marker from subsequent analysis. The number of alleles in the remaining seven microsatellite loci ranged from 8 (Bcal μ 2) to 25 (Bcal μ 3). Diversity measures for microsatellite and MHC loci are given in Table 1 and allele frequencies in Table A in File S1. Almost all of the microsatellite alleles were encountered at least twice, either in the same or in different populations and errors due to PCR or scoring are likely to be small. PCR repeats of individuals never gave conflicting results. Again, diversity was lower in the PGE group than in the REF group. There were 35 population-specific microsatellite alleles out of a total of 118 (30%) across all loci. A total of 52 alleles (44%, range 29–50%) including 26 population-specific alleles (74%) were found only in the REF group and 16 alleles (nine private) only in the PGE group. Across all loci fifty alleles (42%, range 25–50%) occurred in both groups. No microsatellite locus therefore showed allelic differentiation north and south of the Pyrenees as great as that shown by the MHC locus.

Twenty-four of 126 population \times microsatellite loci comparisons showed significant deviations from HWE after Bonferroni correction. In all cases this was due to a homozygote excess and Micro-Checker indicated the possibility of null alleles in several populations at Bcal μ 1, 2, 3, 4 and 6 with estimated frequencies ranging from 0.09 to 0.32 ([85], estimator 1; Table B in File S1). The number of loci with homozygote excess was particularly high in the German and Spanish (Seville) populations. Null alleles may

	1	5	10	15	20	25	30	35	40	45	50	55	60	65	70	75	80	85	90
MEME																			
FUBAR			x	x	*		x	x	x	*		x	x	*	x	x	*	x	x
BC B9	T	A	A	V	D	M	T	E	V	K	S	E	C	H	F	S	N	G	T
BC B12
BC B21	.	.	F
BC B25
BC B42	.	.	E	.	F
BC B1
BB B1	.	.	E	.	F
BB B4	.	.	D	.	Y	.	Q	.	V	.	Q	.	Y	.	S
BB B8
BV 1	.	.	M	.	D	.	Y	.	L

Figure 2. Amino acid alignment of a subset of MHC class II sequences. MHC class II amino acid sequences of *B. calamita* (BC), *B. bufo* (BB) and *B. viridis* (BV). Position 2 is the first amino acid position in exon 2 in these species according to splice site analysis. Position 5 corresponds to the first amino acid position of the second exon in the human MHC locus HLA-DRB. Shaded columns represent putative antigen binding sites (ABS) according to Brown *et al.* (1993) and/or Tong *et al.* (2006). Sign ‘-’ at position 77 denotes a codon deletion; signs ‘x’ and ‘*’ indicate amino acid positions under positive selection as determined by a mixed effects model of evolution (MEME) and a fast unbiased Bayesian approximation (FUBAR), respectively. The positive selection analysis was based on 57 alleles from locus B. doi:10.1371/journal.pone.0100176.g002

therefore be a cause of the deviation from HWE. Another possible explanation is that in some populations a proportion of the samples consisted of siblings, although measures were taken to avoid sampling family groups [50]. However, as this was a small

proportion of the total number of populations we did not exclude these from further analysis (see also [50]).

After Bonferroni corrections there were no cases of linkage disequilibrium among the loci.

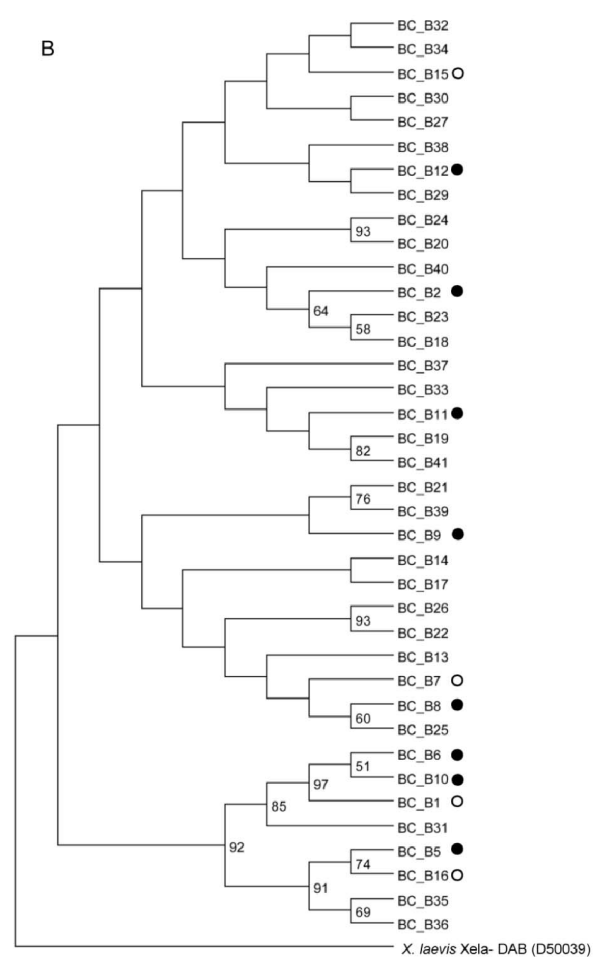
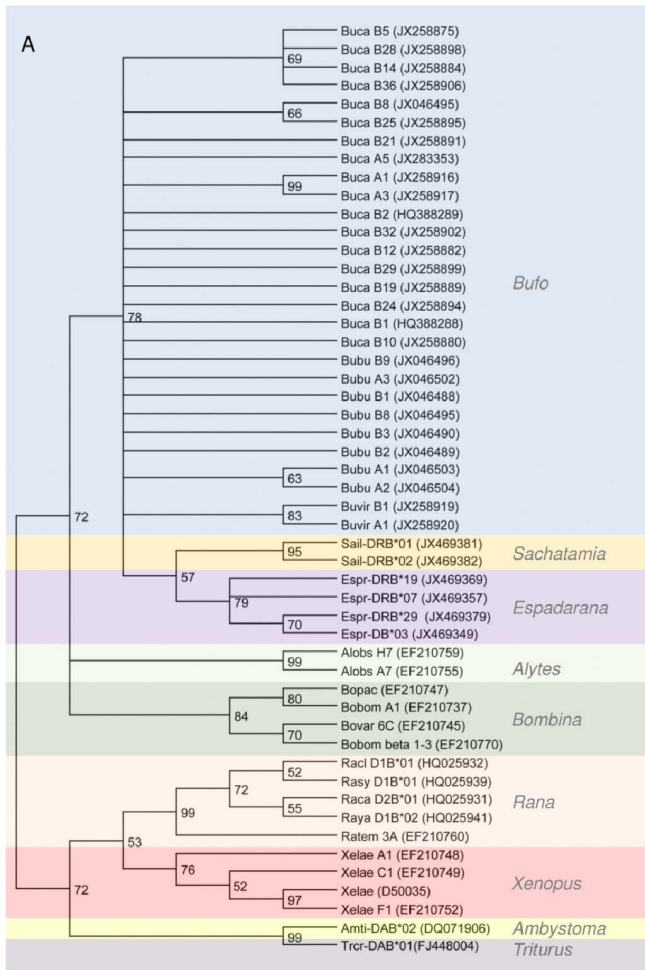


Figure 3. Phylogenetic tree of anuran exon 2 MHC class II nucleotide sequences. A: Multispecies comparisons using 157 bp of sequence. *Triturus* (Trcr) and *Ambystoma* (Amti) sequences were used as outgroups. Genbank accession numbers are given in brackets. B: *B. calamita* alleles with *Xenopus* outgroup using 282 bp of sequence. Filled circles, alleles only found in the PGE; open circles, alleles only found in SW France and PGE. Remaining alleles were only found in the REF populations. A ML bootstrap consensus tree from 1000 replicates [82] was constructed in Mega 5 [60]. The evolutionary distances were computed using the Kimura 2-parameter method [71]. Only bootstrap values above 50% are shown. doi:10.1371/journal.pone.0100176.g003

Comparison of MHC and Microsatellite Variation

For both microsatellite and MHC markers most variation was accounted for at the within-population level (49% and 42% respectively) or among populations within REF and PGE groups (39% and 51% respectively, Table 2). However, the mean number of alleles corrected for sample size (allelic richness, R) was significantly higher in the REF than in the PGE for both microsatellite and MHC loci (MHC: $\chi^2 = 4.20$, $DF = 1$, $P = 0.0404$; microsatellites: $\chi^2 = 6.92$, $DF = 1$, $P = 0.0085$). MHC and microsatellite allelic richness was significantly correlated among populations where both types of loci were sampled (Figure 4A, $r_s = 0.8371$, $n = 15$, $P = 0.0001$). Microsatellite and MHC allelic richness outside Iberia declined with distance from the SW France refugium area (Figure 4B, $r_s = -0.7899$, $n = 14$, $P = 0.0013$). Expected heterozygosity between the types of loci was also significantly correlated (Figure 4C, $r_s = 0.8312$, $n = 15$, $P = 0.0002$). None of the correlations were unduly influenced by populations with a significant amount of null alleles (see Figure 4A and Figure 4C as well as Table A and Table B in File S1) and the correlations between heterozygosity and allelic richness for both types of loci were also significant excluding SW Spain and Germany from the analysis (H_E : $r_s = 0.7552$, $n = 13$, $P = 0.0001$; R : $r_s = 0.7872$, $n = 13$, $P = 0.000$). Average F_{IS} values of MHC and microsatellite loci across all populations in this PGE zone were low in both cases (0.019 and 0.028 respectively) and not significantly different (Wilcoxon signed rank test, $P = 0.603$).

Pairwise F_{ST} comparisons among populations indicated significant population differentiation between 128 of the 136 population comparisons for MHC loci and between all but three for the microsatellite data (see Table S1). Using Mantel tests, pairwise F_{ST} and D_{EST} were significantly intercorrelated both for MHC and microsatellite loci for the PGE region including SW France (MHC: $r_s = 0.6372$, $n = 105$, $P < 0.0001$; microsatellite: $r_s = 0.2548$, $n = 105$, $P = 0.0089$). However, in several cases where geographical separation was high, MHC $D_{EST} = 1$ thus providing incomplete resolution of differentiation level. Subsequent comparisons therefore focused on pairwise F_{ST} estimates which were correlated between MHC and microsatellite loci ($r_s = 0.3128$, $n = 105$, $P = 0.0012$). Excluding Iberian populations, among areas analysed for both microsatellites and MHC genotypes and not separated by seawater ($n = 8$; Bordeaux, SW France; Zurich, Switzerland; Carnac, France; Penmarch, France; Cherbourg, France; Halle, Germany; Bukowno/Bielowieza, Poland; Parnu, Estonia), the correlation between MHC and microsatellite pairwise F_{ST} estimates was also strong ($r_s = 0.432$, $P = 0.025$). Mean pairwise F_{ST} estimates in this region were similar for both types of loci (0.428 for microsatellites, 0.487 for MHC) and there was significant isolation by distance (IBD, $P < 0.0001$ in both cases). However, the strength of IBD was greater for MHC than for microsatellites as shown using untransformed F_{ST} and distance estimates in Figure 5. Regression slopes for the two loci were significantly different ($F = 6.14$, $P = 0.0165$). This strongly indicates a role of selection in shaping MHC diversity, as the effects of drift on microsatellite F_{ST} estimates are expected to be greater than those on MHC loci, due to their higher mutation rates.

Phylogeographic trees based on microsatellite and MHC allele frequencies were broadly congruent (Figure 6). However, allele frequencies and distributions in the PGE region were significantly different between the loci (Figure 7). We excluded colour coding for the MHC locus in the Iberian populations from this comparison, as they do not share any alleles with the other populations and contain a large number of population specific alleles. For a full comparison see Table A in File S1 for allele frequencies at all loci in all populations. Certain MHC alleles were

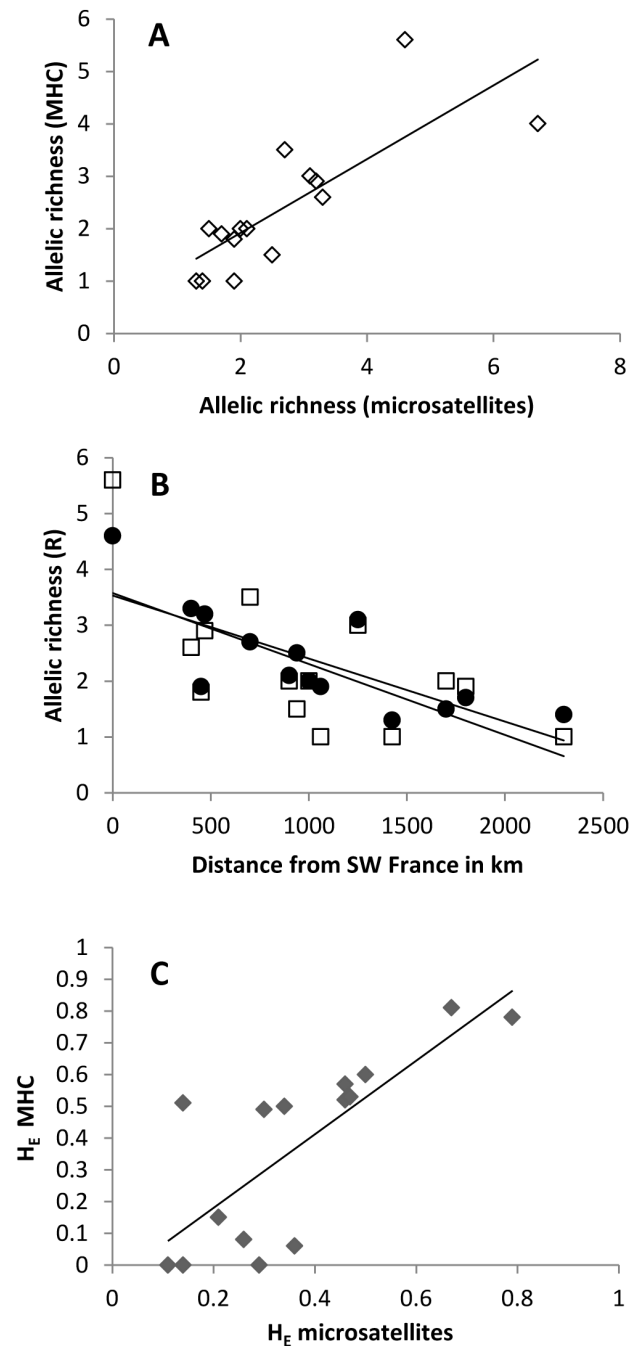


Figure 4. MHC and microsatellite diversity comparisons. A: Correlation of MHC and microsatellite allelic richness (R). B: Microsatellite (\square) and MHC (\bullet) allelic richness (R) and distance from SW France. C: Correlation of MHC and microsatellite expected heterozygosity (H_E). doi:10.1371/journal.pone.0100176.g004

common in adjacent geographic areas (e.g. Buca B2 in Ireland, UK, Netherlands, Germany and Sweden, Buca B5 in Sweden, Denmark, Estonia, Poland, Switzerland and Germany) (Figure 7A). No such pattern could be discerned for the most polymorphic microsatellite locus Bcal μ 3 (Figure 7B).

Table 2. AMOVA results for MHC and microsatellite loci.

	Among groups	Among populations within groups	Within populations
microsatellites	11.86*	39.44*	48.69*
MHC	6.37*	42.38*	51.25 ns

Percentage of variation explained by among group (PGE and REF), among population within groups and within population. Associated significance values of variance components based on 1023 permutations: ns = non significant, * = $P < 0.001$.
doi:10.1371/journal.pone.0100176.t002

Discussion

Nucleotide distances in the MHC locus (0.094) were comparable to those found in other amphibian species, where diversity ranged from 0.062 in *Rana warszewitschii* to 0.155 in *R. catesbeiana* [41], [39], [40]. Many of the positively selected sites we identified in exon 2 corresponded to those involved in peptide binding in equivalent human MHC class II proteins [83], [61]. Many of these sites were congruent with human ABS identified by either Tong *et al.* [61] or Brown *et al.* [83] (Figure 2). The others were located outside the human ABS and some of the human ABSs were not identified as positively selected sites in the *Bufo* MHC class II loci. Similar findings have been reported by others (e.g. [86], [87], [84], [41]), indicating that species-specific selection pressures were acting on the MHC genes. Two methods for detecting recombination in the *Bufo* MHC sequences indicated its occurrence in these species. This may explain the adjacent intron 2 sequence similarity found at locus A and B within *B. calamita* [43]. Although our phylogenetic analysis was based on only a short DNA sequence, it does reflect the current view of the phylogenetic relationship of amphibians [88], [89], [90]. Interestingly the Central American glass frog *Espadarana prosoblepon*, which clustered with *Bufo* in our phylogenetic tree, also showed remarkable sequence similarity to *Bufo* MHC sequences in the first 200 bp of intron 2, which basically consists of a 100 bp repeat [43], [44]. Although we did not sequence intron 2 of *B. viridis* or *B. bufo* the fact that the intron-specific primers amplify MHC loci in these species indicates at least some conservation at introns across taxa [43]. Blast searches did not find these sequences elsewhere. Such conservation across widely separate taxa may indicate some functional significance of this sequence. For example, the first

130 bp of intron 2 sequences of New World ranid species (*Rana catesbeiana*, *R. clamitans*, *R. pipiens*, *R. sylvatica*, *R. yavapaiensis*, *R. warszewitschii*, *R. palustris*; [41]) were also remarkably conserved across species, though no repeat was detected. Sato *et al.* [91] analysed 114 intron 2 sequences of passerine bird species and found that most of them largely consisted of repeat sequences, with a 10 bp repeat being particularly common. In addition they found a 60–80 bp DNA segment in intron 2 that occurred in noncoding segments of MHC sequences in a number of other passerine bird species. The function or role of repetitive sequences or conserved elements in intron 2 is not yet clear but clearly requires further study.

Of particular interest within the *B. calamita* MHC were alleles (all in Iberian REF populations) that had a codon deletion at the same position as found in the great crested newt *Triturus cristatus* in Romanian REF populations [12] as well as in the glass frog *Espadama prosoblepon* (Espr-DRB*26, [44]) in Central America. It may be that selection pressure in colder climates eliminated these alleles from populations in North European amphibians, or that they confer advantages in warmer climates. The loss of these alleles by drift as populations expanded north cannot be ruled out but seems a remarkable coincidence for two unrelated taxa.

There was a clear difference in the levels of both MHC and microsatellite diversity between the REF and the PGE populations of *B. calamita*. The lack of shared MHC alleles between the REF and PGE populations was surprising and it is possible more shared alleles may be found in other REF populations. Nevertheless, for comparison, Babik *et al.* [12] found that populations of the great crested newt (*Triturus cristatus*) in post glacial expansion (PGE) areas possessed a subset of alleles from the refugia (REF) populations, when they compared three PGE populations from across Europe to only four small REF populations from Romania. Our data support the theory that natterjack toads survived the Weichselian glacial maximum 20 000 years BP in at least one north European refuge, most likely in France, and colonized northern Europe from there [50]. In *B. calamita* and *T. cristatus* variation of microsatellite and MHC loci was high in the REF groups and much lower in the PGE groups. A decrease in allelic diversity from southern to northern Europe is well documented in neutral loci (e.g. [92]). The high similarity in diversity distribution (decreasing in the PGE area as a function of distance from the REF area) and in phylogeographic patterns between the two types of loci imply that drift rather than selection was the dominant influence on MHC allelic variation at the biogeographic range scale. Mean F_{ST} estimates were close to zero for both classes of loci, with no signal of heterozygote excess as an indicator of diversifying selection in the MHC locus. A recent meta-analysis of the roles of natural selection and genetic drift in shaping MHC variation concluded that selection combined with drift during population bottlenecks can result in loss of MHC polymorphism at even greater rates than neutral genetic diversity [93]. Other studies have shown that microsatellite and MHC diversity is lost in similar proportions over time, with balancing selection unable to mitigate genetic drift [94]

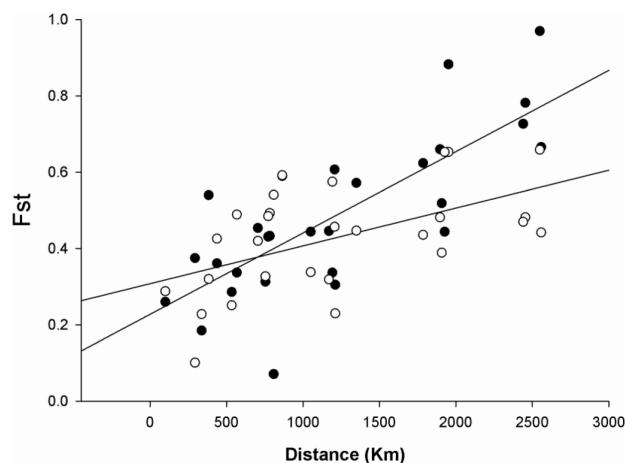


Figure 5. Relationships of pairwise F_{ST} and distance estimates. Microsatellite data are represented by open circles and MHC data by filled circles.
doi:10.1371/journal.pone.0100176.g005

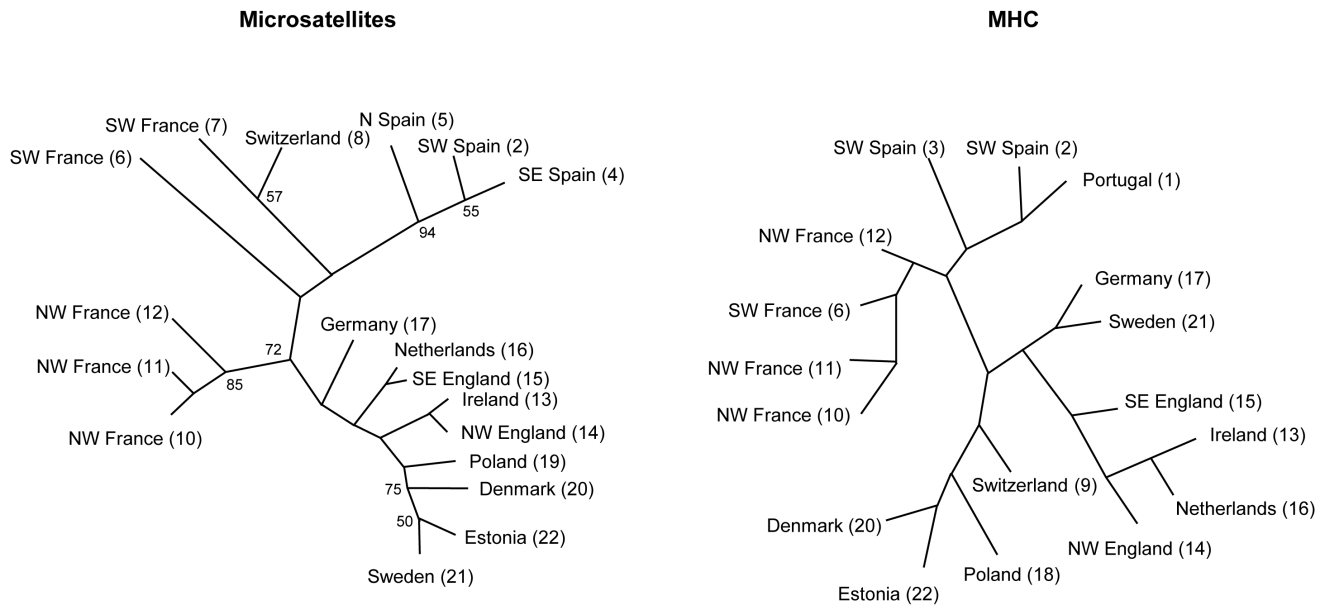


Figure 6. Phylogeography of *B. calamita* populations. Bootstrap values >50% are given for the microsatellite analysis. Sampling site numbers corresponding to Figure 1 are given in brackets. doi:10.1371/journal.pone.0100176.g006

and that MHC diversity declines more steeply than microsatellite diversity after a bottleneck [95]. However, inconsistencies remain and in some cases selection can maintain polymorphism at MHC loci during population bottlenecks (e.g. [96]).

When comparing two different marker systems such as MHC loci and microsatellites it is important to consider the potential differences in the ages of observed alleles due to the higher mutation rates of microsatellites and potential back mutations. Microsatellite mutation rates in *B. calamita* have been estimated at a relatively low 1×10^{-5} [50], whereas the mutation rate at the DRB1 locus in chimpanzees is estimated to be 1.31×10^{-9} per site per year [97]. Assuming a similar mutation rate for the MHC locus B in *B. calamita* this would give a mutation rate of 1.1×10^{-6} for 279 bp of exon 2 per generation (three years), not much

different from that of the microsatellites. Microsatellite mutation rates increase with microsatellite length and contractions become more likely than expansions as length increases [98]. As natterjack microsatellite length was generally higher in the PGE than in the REF area [50] it is possible that some variation was masked by back mutations generating homoplasy. However, the natterjack microsatellites were relatively short (mostly around 10–20 repeats with a maximum of 29 for Bcal μ 3) and significant homoplasy was considered unlikely.

Despite the likely dominance of drift effects on *B. calamita* MHC variation across the species' range there were some interesting differences between MHC and microsatellite genotype distributions that may imply an additional, albeit minor role of selection in structuring the MHC locus at this large geographical scale. MHC

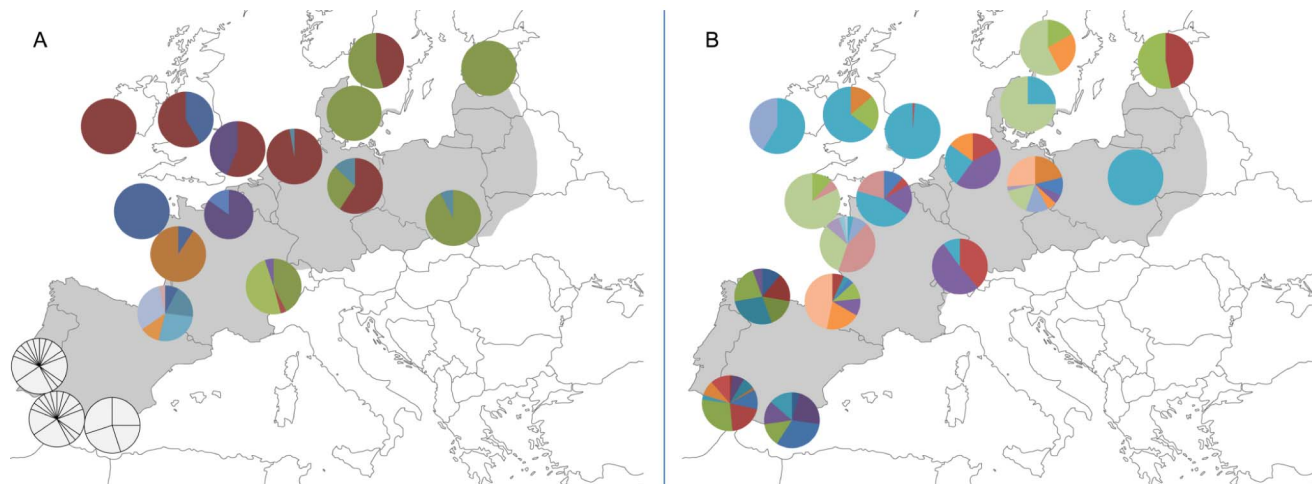


Figure 7. Allele frequency distributions in the PGE area. A: MHC locus allele frequency distributions. Colour coding for the Iberian populations is excluded from this figure due to the large number of population specific alleles present; B: Bcal μ 3 locus allele frequency distributions. Maps modified from d-maps.com. doi:10.1371/journal.pone.0100176.g007

alleles were more sharply differentiated between the REF and PGE regions than were the microsatellite alleles. Isolation by distance effects in those parts of the mainland Europe PGE area where gene flow remained possible after postglacial sea level rise was significantly stronger for the MHC than for the microsatellite loci. The commonest MHC alleles in the PGE group were, on average, at higher frequency and more geographically clustered than the commonest alleles in the microsatellite locus with the most comparable allelic diversity. This pattern difference might imply weak effects of selection reflected in patterns of common MHC allele abundance in specific regions, such as north-west France, north-central Europe and eastern Europe, perhaps in turn reflecting local differences in pathogen communities. Pathogens often exhibit a 'latitudinal diversity gradient', with high diversity at the equator decreasing towards the poles [99]. For example, temperature is an indirect selective mechanism maintaining MHC diversity in wild salmon [18]. Therefore it is possible that the higher MHC diversity in the southern populations of *B. calamita* is maintained by higher pathogen-mediated selection pressure, but further studies into actual difference of pathogen prevalence in the various regions are needed to test this hypothesis.

Overall, our evidence clearly implies a stronger influence of drift than selection on this *B. calamita* MHC locus at the biogeographical scale. This is essentially similar to the situation discovered with a comparable study of another widespread European amphibian, *Triturus cristatus* [12]. Comparison of MHC and neutral loci in four populations of Atlantic herring (*Clupea harengus*) also failed to detect any evidence of selection acting on the MHC locus, although in this study a MHC-embedded microsatellite locus was used and it is not clear to what extent this reflected variability in the exon [100]. Marsden *et al.* [24] also found that although microsatellite diversity and MHC diversity were correlated in African wild dog populations, indicating genetic drift to be a major influencing factor, there were signatures of selection at the MHC locus. The apparent weakness of selective effects may however be influenced by the scale of the study. In Atlantic salmon drift and migration were more important than selection on large geographical scales but at smaller geographical scales the influence of selection was detected at MHC loci [101]. Postglacial colonisation with associated bottlenecks can evidently leave strong signatures of genetic drift long after the event. In contrast to this, the same MHC locus in a *B. bufo* population translocated over 400 km within the UK adapted within three generations to an allele frequency distribution similar to that of neighbouring populations in the receptor area [102], presumably reflecting selection in favour of the new conditions. A recent phylogeographic study of the bank vole (*Myodes glareolus*) found no spatial genetic structure among populations at MHC loci, but clear differentiation

reflecting their major glacial refugia at a mtDNA gene. This may indicate yet another situation in which spatiotemporal variations in selection pressures acting over large areas can mask historical signals of population origins [103]. Other studies have also indicated that the mode and strength of selection acting on MHC diversity varies in time and space [104]. Further studies at small geographical scales including experimental translocations may prove fruitful in the investigation of selection on adaptive variation such as that expected with MHC loci, whilst no doubt further investigations into the role of pathogens in shaping MHC diversity remain necessary in isolating the evolutionary forces shaping MHC diversity.

Supporting Information

Figure S1 Phylogenetic network of MHC class II beta exon 2 sequences. Neighbor-Net tree based on Jukes-Cantor distances of 282 bp of sequence of MHC locus B from *B. calamita*. (TIF)

Table S1 Population differentiation as estimated by F_{ST} values. Numbers in brackets refer to population numbers in Figure 1. Non-significant values are indicated in red italics. A: Population differentiation as estimated by F_{ST} values for MHC data. P-values obtained after: 2720 permutations. Indicative adjusted nominal level (5%) for multiple comparisons is: 0.000368. B: Population differentiation as estimated by F_{ST} values for microsatellite data, based on 7 loci. P-values obtained after: 3060 permutations. Indicative adjusted nominal level (5%) for multiple comparisons is: 0.000327. (XLSX)

File S1 Table A (sheet 1): Allelic frequencies in each population for microsatellite and MHC loci. Numbers in brackets refer to population numbers in Figure 1. Table B (sheet two): Brookfield I estimates of null allele frequencies at microsatellite loci. (XLSX)

Acknowledgments

Thanks to those who provided samples in the earlier studies and to Benedikt Schmidt (Switzerland), Miguel Tejado (Spain), Mirjam van de Vliet (Portugal), Wieslaw Babik and Maciej Bonk (Poland) for providing new samples for the present work. We also thank the anonymous reviewers for their valuable feedback.

Author Contributions

Conceived and designed the experiments: IZ TJCB. Performed the experiments: IZ. Analyzed the data: IZ. Contributed reagents/materials/analysis tools: TJCB. Wrote the paper: IZ TJCB.

References

- Klein J, Sato A (1998) Birth of the major histocompatibility complex. *Scandinavian Journal of Immunology* 47: 199–209.
- Kobari F, Kasahara M, Tochinai S (1995) Structure and evolution of *Xenopus laevis* MHC class II beta-chain gene. *Zoological Science (Tokyo)* 12: 38.
- Kobari F, Sato K, Shum BP, Tochinai S, Katagiri M, et al. (1995) Exon-intron organization of *Xenopus* MHC class-II beta-chain genes. *Immunogenetics* 42: 376–385.
- Hedrick PW (1994) Evolutionary genetics of the major histocompatibility complex. *American Naturalist* 143: 945–964.
- Garrigan D, Hedrick PW (2003) Perspective: detecting adaptive molecular polymorphism: lessons from the MHC. *Evolution* 57: 1707–1722.
- Langefors A, Lohm J, Grahn M, Andersen O, von Schantz T (2001) Association between major histocompatibility complex class IIB alleles and resistance to *Aeromonas salmonicida* in Atlantic salmon. *Proceedings of the Royal Society of London Series B-Biological Sciences* 268: 479–485.
- Meyer-Lucht Y, Sommer S (2005) MHC diversity and the association to nematode parasitism in the yellow-necked mouse (*Apodemus flavicollis*). *Molecular Ecology* 14: 2233–2244.
- Froeschke G, Sommer S (2005) MHC Class II DRB variability and parasite load in the striped mouse (*Rhabdomys pumilio*) in the southern Kalahari. *Molecular Biology and Evolution* 22: 1254–1259.
- Simkova A, Ottova E, Morand S (2006) MHC variability, life-traits and parasite diversity of European cyprinid fish. *Evolutionary Ecology* 20: 465–477.
- Cheng Y, Sanderson C, Jones M, Belov K (2012) Low MHC class II diversity in the Tasmanian devil (*Sarcophilus harrisi*). *Immunogenetics* 64: 525–533.
- Hedrick PW (2001) Conservation genetics: where are we now? *Trends in Ecology and Evolution* 16: 629–636.
- Babik W, Pabijan M, Arntzen JW, Cogalniceanu D, Durka W, et al. (2009) Long-term survival of a urodele amphibian despite depleted major histocompatibility complex variation. *Molecular Ecology* 18: 769–781.
- Ellegren H, Hartman G, Johansson M, Andersson L (1993) Major histocompatibility complex monomorphism and low levels of DNA fingerprinting variability in a reintroduced and rapidly expanding population of beavers. *Proceedings of the National Academy of Sciences of the USA* 90: 8150–8153.

14. Piertney SB, Oliver MK (2005) The evolutionary ecology of the major histocompatibility complex. *Heredity* 96: 7–21.
15. Bonneaud C, Perez-Tris J, Federici P, Chastel O, Sorci G (2006) Major histocompatibility alleles associated with local resistance to malaria in a passerine. *Evolution* 60: 383–389.
16. Sommer S (2005) The importance of immune gene variability (MHC) in evolutionary ecology and conservation. *Frontiers in Zoology* 2: 16.
17. Wegner KM, Reusch TBH, Kalbe M (2003) Multiple parasites are driving major histocompatibility complex polymorphism in the wild. *Journal of Evolutionary Biology* 16: 224–232.
18. Dionne M, Miller KM, Dodson JJ, Caron F, Bernatchez L (2007) Clinal variation in MHC diversity with temperature: evidence for the role of host–pathogen interaction on local adaptation in Atlantic salmon. *Evolution* 61: 2154–2164.
19. de Bellocq JG, Charbonnel N, Morand S (2008) Coevolutionary relationship between helminth diversity and MHC class II polymorphism in rodents. *Journal of Evolutionary Biology* 21: 1144–1150.
20. Campos JL, Posada D, Moran P (2006) Genetic variation at MHC, mitochondrial and microsatellite loci in isolated populations of Brown trout (*Salmo trutta*). *Conservation Genetics* 7: 515–530.
21. Zeisset I, Beebee TJC (2010) Larval fitness, microsatellite diversity and MHC class II diversity in common frog (*Rana temporaria*) populations. *Heredity* 104: 423–430.
22. Ploshnitsa AI, Goltsman ME, Macdonald DW, Kennedy LJ, Sommer S (2012) Impact of historical founder effects and a recent bottleneck on MHC variability in commander arctic foxes (*Vulpes lagopus*). *Ecology and Evolution* 2: 165–180.
23. Shafer ABA, Fan CW, Côté SD, Coltman DW (2012) (Lack of) Genetic diversity in immune genes predates glacial isolation in the North American mountain goat (*Oreamnos americanus*). *Journal of Heredity* 103: 371–379.
24. Marsden CD, Woodroffe R, Mills MGL, McNutt JW, Creel S, et al. (2012) Spatial and temporal patterns of neutral and adaptive genetic variation in the endangered African wild dog (*Lycaon pictus*). *Molecular Ecology* 21: 1379–1393.
25. Lillie M, Woodward RE, Sanderson CE, Eldridge MDB, Belov K (2012) Diversity at the major histocompatibility complex class II in the platypus, *Ornithorhynchus anatinus*. *Journal of Heredity* 103: 467–478.
26. Osborne AJ, Zavodna M, Chilvers BL, Robertson BC, Negro SS, et al. (2013) Extensive variation at MHC DRB in the New Zealand sea lion (*Phocastor hookeri*) provides evidence for balancing selection. *Heredity* 111: 44–56.
27. Zeisset I, Beebee TJC (2008) Amphibian phylogeography: a model for understanding historical aspects of species distributions. *Heredity* 101: 109–119.
28. Stuart SN, Chanson JS, Cox NA, Young BE, Rodrigues ASL, et al. (2004) Status and trends of amphibian declines and extinctions worldwide. *Science* 306: 1783–1786.
29. Beebee TJC, Griffiths RA (2005) The amphibian decline crisis: A watershed for conservation biology? *Biological Conservation* 125: 271–285.
30. Houlahan JE, Findlay CS, Schmidt BR, Meyer AH, Kuzmin SL (2000) Quantitative evidence for global amphibian population declines. *Nature* 404: 752–755.
31. Fisher MC, Garner TWJ, Walker SF (2009) Global Emergence of *Batrachochytrium dendrobatidis* and amphibian chytridiomycosis in space, time, and host. *Annual Review of Microbiology* 63: 291–310.
32. Walker SF, Bosch J, Gomez V, Garner TWJ, Cunningham AA, et al. (2010) Factors driving pathogenicity vs. prevalence of amphibian panzootic chytridiomycosis in Iberia. *Ecology Letters* 13: 372–382.
33. Hidalgo-Vila J, Diaz-Paniagua C, Marchand MA, Cunningham AA (2012) *Batrachochytrium dendrobatidis* infection of amphibians in the Doñana National Park, Spain. *Diseases of Aquatic Organisms* 98: 113–119.
34. Gahl MK, Longcore JE, Houlahan JE (2012) Varying responses of northeastern North American amphibians to the chytrid pathogen *Batrachochytrium dendrobatidis*. *Conservation Biology* 26: 135–141.
35. Searle CL, Gervasi SS, Hua J, Hammond JI, Relyea RA, et al. (2011) Differential host susceptibility to *Batrachochytrium dendrobatidis*, an emerging amphibian pathogen. *Conservation Biology* 25: 965–974.
36. Hughes AL, Yeager M (1998) Natural selection at major histocompatibility complex loci of vertebrates. *Annual Review of Genetics* 32: 415–435.
37. Richmond JQ, Savage AE, Zamudio KR, Rosenblum EB (2009) Toward immunogenetic studies of amphibian chytridiomycosis: linking innate and acquired immunity. *Bioscience* 59: 311–320.
38. Savage AE, Zamudio KR (2011) MHC genotypes associate with resistance to a frog-killing fungus. *Proceedings of the National Academy of Sciences of the USA* 108: 16705–16710.
39. Hauswaldt JS, Stuckas H, Pfautsch S, Tiedemann R (2007) Molecular characterization of MHC class II in a nonmodel anuran species, the fire-bellied toad *Bombina orientalis*. *Immunogenetics* 59: 479–491.
40. Zeisset I, Beebee TJC (2009) Molecular characterization of major histocompatibility complex class II alleles in the common frog, *Rana temporaria*. *Molecular Ecology Resources* 9: 738–745.
41. Kiemnec-Tyburczy KM, Richmond JQ, Savage AE, Zamudio KR (2010) Selection, trans-species polymorphism, and locus identification of major histocompatibility complex class II beta alleles of New World ranid frogs. *Immunogenetics* 62: 741–751.
42. May S, Beebee TJC (2009) Characterisation of major histocompatibility complex class II alleles in the natterjack toad, *Bufo calamita*. *Conservation Genetics Resources* 1: 415–417.
43. Zeisset I, Beebee TJC (2013) *Bufo* MHC class II loci with conserved introns flanking exon 2: cross-species amplification with common primers. *Conservation Genetics Resources* 5: 211–213.
44. Kiemnec-Tyburczy KM, Zamudio KR (2012) Novel locus-specific primers for major histocompatibility complex class II alleles from glass frogs developed via genome walking. *Conservation Genetics Resources* 5: 109–111.
45. Babik W, Pabijan M, Radwan J (2008) Contrasting patterns of variation in MHC loci in the Alpine newt. *Molecular Ecology* 17: 2339–2355.
46. Sato K, Flajnik MF, du Pasquier L, Katagiri M, Kasahara M (1993) Evolution of the Mhc - isolation of class-II beta-chain cDNA clones from the amphibian *Xenopus laevis*. *Journal of Immunology* 150: 2831–2843.
47. Laurens V, Chapusot C, Ordonez MD, Bentrafi F, Padros MR, et al. (2001) Axolotl MHC class II beta chain: predominance of one allele and alternative splicing of the beta 1 domain. *European Journal of Immunology* 31: 506–515.
48. Bos DH, DeWoody JA (2005) Molecular characterization of major histocompatibility complex class II alleles in wild tiger salamanders (*Ambystoma tigrinum*). *Immunogenetics* 57: 775–781.
49. Ohta Y, Goetz W, Hossain MZ, Nonaka M, Flajnik MF (2006) Ancestral organization of the MHC revealed in the amphibian *Xenopus*. *Journal of Immunology* 176: 3674–3685.
50. Rowe G, Harris DJ, Beebee TJC (2006) Lusitania revisited: A phylogeographic analysis of the natterjack toad *Bufo calamita* across its entire biogeographical range. *Molecular Phylogenetics and Evolution* 39: 335–346.
51. Beebee TJC, Rowe G (2000) Microsatellite analysis of natterjack toad *Bufo calamita* Laurenti populations: consequences of dispersal from a Pleistocene refugium. *Biological Journal of the Linnean Society* 69: 367–381.
52. Sunnucks P, Wilson ACC, Beheregaray LB, Zenger K, French J, et al. (2000) SSCP is not so difficult: the application and utility of single-stranded conformation polymorphism in evolutionary biology and molecular ecology. *Molecular Ecology* 9: 1699–1710.
53. Van Oosterhout C, Hutchinson WF, Wills PM, Shipley P (2004) MICROCHECKER: software for identifying and correcting genotyping errors in microsatellite data. *Molecular Ecology Notes* 4: 535–538.
54. Beaumont MA, Nichols RA (1996) Evaluating loci for use in the genetic analysis of population structure. *Proceedings of the Royal Society of London Series B: Biological Sciences* 263: 1619–1626.
55. Antao T, Lopes A, Lopes RJ, Beja-Pereira A, Luikart G (2008) LOSITAN: A webbench to detect molecular adaptation based on a F(st)-outlier method. *BMC Bioinformatics* 9: 323.
56. Reese MG, Eeckman FH, Kulp D, Haussler D (1997) Improved splice site detection in Genie. *Journal of Computational Biology* 4: 311–323.
57. Hall TA (1999) BioEdit: a user-friendly biological sequence alignment editor and analysis program for Windows 95/98/NT. *Nucleic Acids Symposium Series* 41: 95–98.
58. Nei M, Gojobori T (1986) Simple methods for estimating the numbers of synonymous and nonsynonymous nucleotide substitutions. *Molecular Biology and Evolution* 3: 418–426.
59. Jukes TH, Cantor CR (1969) Evolution of protein molecules. In: Munro HN (ed.), *Mammalian protein metabolism*, Academic Press, New York, 21–132.
60. Tamura K, Peterson D, Peterson N, Stecher G, Nei M, et al. (2011) MEGA5: Molecular evolutionary genetics analysis using maximum likelihood, evolutionary distance, and maximum parsimony methods. *Molecular Biology and Evolution* 28: 2731–2739.
61. Tong JC, Bramson J, Kanduc D, Chow S, Sinha AA, et al. (2006) Modelling the bound conformation of *Pemphigus vulgaris*-associated peptides to MHC Class II DR and DQ alleles. *Immunome Research* 2: 1–10.
62. Nei M, Kumar S (2000) *Molecular evolution and phylogenetics*. Oxford University Press, New York.
63. Zuckerkandl E, Pauling L (1965) Evolutionary divergence and convergence in proteins. In: Bryson V, Vogel HJ (eds.) *Evolving genes and proteins*, Academic Press, New York, 97–166.
64. Murrell B, Wertheim JO, Moola S, Weighill T, Scheffler K, et al. (2012) Detecting individual sites subject to episodic diversifying selection. *PLoS Genetics* 8: e1002764.
65. Delpont W, Poon AF, Frost SDW, Kosakovsky Pond SL (2010) Datamonkey 2010: a suite of phylogenetic analysis tools for evolutionary biology. *Bioinformatics* 26: 2455–2457.
66. Padidam M, Sawyer S, Fauquet CM (1999) Possible emergence of new geminiviruses by frequent recombination. *Virology* 265: 218–225.
67. Smith JM (1992) Analyzing the mosaic structure of genes. *Journal of Molecular Evolution* 34: 126–129.
68. Martin DP, Lemey P, Lott M, Moulton V, Posada D, et al. (2010) RDP3: a flexible and fast computer program for analyzing recombination. *Bioinformatics* 26: 2462–2463.
69. Posada D (2002) Evaluation of methods for detecting recombination from DNA sequences: Empirical data. *Molecular Biology and Evolution* 19: 708–717.
70. Kosakovsky Pond SL, Posada D, Gravenor MB, Woelk CH, Frost SDW (2006) Automated phylogenetic detection of recombination using a genetic algorithm. *Molecular Biology and Evolution* 23: 1891–1901.

71. Kimura M (1980) A simple method for estimating evolutionary rates of base substitutions through comparative studies of nucleotide-sequences. *Journal of Molecular Evolution* 16: 111–120.
72. Felsenstein J (1985) Confidence-limits on phylogenies - an approach using the bootstrap. *Evolution* 39: 783–791.
73. Bryant D, Mouton V (2004) Neighbor-net: an agglomerative method for the construction of phylogenetic networks. *Molecular Biology and Evolution* 21: 255–265.
74. Hudson DH, Bryant D (2006) Application of phylogenetic networks in evolutionary studies. *Molecular Biology and Evolution* 23: 254–267.
75. Raymond M, Rousset F (1995) Genepop (Version 1.2) Population genetics software for exact tests and ecumenicism. *Journal of Heredity* 86: 248–249.
76. Weir BS, Cockerham CC (1984) Estimating F-Statistics for the analysis of population-structure. *Evolution* 38: 1358–1370.
77. Goudet J (1995) FSTAT (Version 1.2): A computer program to calculate F-statistics. *Journal of Heredity* 86: 485–486.
78. Jost L (2008) G_{ST} and its relatives do not measure differentiation. *Molecular Ecology* 17: 4015–4026.
79. Peakall R, Smouse PE (2006) GENALEX 6: genetic analysis in Excel. Population genetic software for teaching and research. *Molecular Ecology Notes* 6: 288–295.
80. Peakall R, Smouse PE (2012) GenAEx 6.5: genetic analysis in Excel. Population genetic software for teaching and research – an update. *Bioinformatics* 28: 2537–2539.
81. Excoffier L, Lischer HEL (2010) Arlequin suite ver 3.5: A new series of programs to perform population genetics analyses under Linux and Windows. *Molecular Ecology Resources* 10: 564–567.
82. Felsenstein J (1993) PHYLIP (Phylogeny inference package). Version 3.5C. Department of Genetics, University of Washington, Seattle.
83. Brown JH, Jardetzky TS, Gorga JC, Stern LJ, Urban RG, et al. (1993) Three-dimensional structure of the human class-II histocompatibility antigen HLA-DR1. *Nature* 364: 33–39.
84. Babik W (2009) Methods for MHC genotyping in non-model vertebrates. *Molecular Ecology Resources* 10: 237–251.
85. Brookfield JFY (1996) A simple new method for estimating null allele frequency from heterozygote deficiency. *Molecular Ecology* 5: 453–455.
86. Meyer-Lucht Y, Otten C, Puettker T, Sommer S (2008) Selection, diversity and evolutionary patterns of the MHC class II DAB in free-ranging neotropical marsupials. *BMC Genetics* 9: 39.
87. Schad J, Dechmann DKN, Voigt CC, Sommer S (2011) MHC class II DRB diversity, selection pattern and population structure in a neotropical bat species, *Noctilio albiventris*. *Heredity* 107: 115–126.
88. Pyron RA, Wiens JJ (2011) A large scale phylogeny of Amphibia including over 2800 species, and a revised classification of extant frogs, salamanders, and caecilians. *Molecular Phylogenetics and Evolution* 61: 543–583.
89. Graybeal A (1997) Phylogenetic relationships of bufonid frogs and tests of alternate macroevolutionary hypotheses characterizing their radiation. *Zoological Journal of the Linnean Society* 119: 297–338.
90. Frost DR, Grant T, Fivovich J, Bain RH, Haas A, et al. (2006) The Amphibian tree of life. *Bulletin of the American Museum of Natural History* 297: 1–370.
91. Sato A, Tichy H, Grant PR, Grant BR, Sato T, et al. (2011) Spectrum of MHC class II variability in Darwin's finches and their close relatives. *Molecular Biology and Evolution* 28: 1943–1956.
92. Hewitt GM (1999) Post-glacial re-colonization of European biota. *Biological Journal of the Linnean Society* 68: 87–112.
93. Sutton J T, Nakagawa S, Robertson BC, Jamieson IG (2011) Disentangling the roles of natural selection and genetic drift in shaping variation at MHC immunity genes. *Molecular Ecology* 20: 4408–4420.
94. Taylor SS, Jenkins D, Arcese P (2012) Loss of MHC and neutral variation in Peary caribou: genetic drift is not mitigated by balancing selection or exacerbated by MHC allele distributions. *PLOS ONE* 7(5): e36748.
95. Eimes JA, Bollmer JL, Whittingham LA, Johnson JA, van Oosterhout C, et al. (2011) Rapid loss of MHC class II variation in a bottlenecked population is explained by drift and loss of copy number variation. *Journal of Evolutionary Biology* 24: 1847–1856.
96. Oliver MK, Piertney SB (2012) Selection maintains MHC diversity through a natural population bottleneck. *Molecular Biology and Evolution* 29: 1713–1720.
97. Ohashi J, Naka I, Toyoda A, Takasu M, Tokunaga K, et al. (2006) Estimation of the species-specific mutation rates at the DRB1 locus in humans and chimpanzee. *Tissue Antigens* 68: 427–431.
98. Whittaker JC, Harbord RM, Boxall N, Mackay I, Dawson G, et al. (2003) Likelihood-based estimation of microsatellite mutation rates. *Genetics* 164: 781–787.
99. Guernier V, Mochberg ME, Guégan J-F (2004) Ecology drives the worldwide distribution of human diseases. *PLOS Biology*. 2: 0740–0746.
100. André C, Larsson LC, Laikre L, Bekkevold D, Brigham J, et al. (2011) Detecting population structure in a high gene-flow species, Atlantic herring (*Clupea harengus*): direct, simultaneous evaluation of neutral vs. putatively selected loci. *Heredity* 106: 270–280.
101. Landry C, Bernatchez L (2001) Comparative analysis of population structure across environments and geographical scales at major histocompatibility complex and microsatellite loci in Atlantic salmon (*Salmo salar*). *Molecular Ecology* 10: 2525–2539.
102. Zeisset I, Beebee TJC (2012) Donor population size rather than local adaptation can be a key determinant of amphibian translocation success. *Animal Conservation* 16: 359–366.
103. Malé P-JG, Martin J-F, Galan M, Deffontaine V, Bryja J, et al. (2012) Discongruence of *Mhc* and cytochrome *b* phylogeographical patterns in *Myodes glareolus* (Rodentia: Cricetidae). *Biological Journal of the Linnean Society* 105: 881–899.
104. Oliver MK, Lambin X, Cornulier T, Piertney S (2009) Spatio-temporal variation in the strength and mode of selection acting on major histocompatibility complex diversity in water vole (*Arvicola terrestris*) metapopulations. *Molecular Ecology* 18: 80–92.